IN SITU CONSTRAINTS ON THE ^{60}FE ABUNDANCE IN THE EARLY SOLAR SYSTEM. J. Kodolányi[1], P. Hoppe[1], and C. Vollmer[2], [1]Max Planck Institute for Chemistry (Hahn-Meitner-Weg 1, 55128 Mainz, Germany; j.kodolanyi@mpic.de), [2]University of Münster, Institute for Mineralogy (Corrensstrasse 24, 48149 Münster, Germany).

Introduction: The abundance of the short-lived radioactive isotope ^{60}Fe (t½ ~2.6 million years; [1]) in the early solar system has been the subject of intense research, as it is relevant for models exploring the evolution of early solar system planetary bodies, and the provenance of the short-lived isotopes present in the early solar system. Based mostly on nickel isotope data from bulk eucrites and quenched angrites, [2] have estimated that the solar system's ^{60}Fe/^{56}Fe ratio at the time canonical calcium-aluminum-rich inclusions (CCAIs; [3]) formed, ^{60}Fe/^{56}Fe$_{CCAI}$, was 1.0 (± 0.1) × 10^{-8} (all uncertainties represent 68 % confidence level, unless stated otherwise). Steele et al. [4] gave a less certain, but higher, estimate of 7.5 (± 3.3) × 10^{-8}, based on ^{60}Ni-deficits in the nickel-rich IVB iron meteorites relative to their isotopically closest undifferentiated counterparts. In contrast to the ^{60}Fe/^{56}Fe$_{CCAI}$ ratios inferred from bulk nickel isotope data, those estimated based on in situ measurements have a greater scatter, and, notably, extend to orders of magnitude higher values, than the above estimates. The highest inferred ^{60}Fe/^{56}Fe$_{CCAI}$ ratio is 1.31 (± 0.23) × 10^{-6} [5]. Most in situ measurements were carried out using SIMS, or the NanoSIMS, on enstatite found in the chondrules of unequilibrated ordinary chondrites (UOCs), because of their high Fe/Ni ratios (up to ~12,000). Some were performed on troilites (which have even higher Fe/Ni ratios), and also yielded high estimated ^{60}Fe/^{56}Fe ratios at the time of formation (0.92 ± 0.12 × 10^{-6}; [6]; ^{60}Fe/^{56}Fe$_{CCAI}$ ratios could not be estimated). The reasons behind the difference between bulk and in situ results are not clear. Insufficient interference correction of in situ data [7], and the effects of aqueous alteration and metamorphic re-equilibration on bulk, as well as in situ measurements have been suggested [8].

Recently, we have been trying to constrain the ^{60}Fe/^{56}Fe ratio of primitive solar system materials at the time of their formation, by using higher spatial resolution in situ isotope analysis than possible before (2–3 µm vs. >10 µm). The improved spatial resolution helps to avoid cracks and inclusions. With the new isotope data, and the nanoscale investigation of potential alteration effects by transmission electron microscopy (TEM) of focused ion beam-prepared samples, we hope to understand the discrepancy between the results of previous in situ and bulk nickel isotope studies. During our first efforts on troilite from the Semarkona and Dominion Range 08006 chondrites [9], we found no significant enrichment in ^{60}Ni from ^{60}Fe decay, despite sometimes extremely high Fe/Ni ratios (^{56}Fe/^{62}Ni ≈ 10^7; note that such high ratios were reported in our poster only). Thus, our troilite data did not support those of [6] (see above).

Here we present the results of our new in situ measurements of the nickel isotope composition and Fe/Ni ratios of silicates from the carbonaceous chondrite Allan Hills A77307 (ALHA77307; CO3), as well as the UOCs Meteorite Hills 00526 (MET 00526; L/LL 3.05), and Queen Alexandra Range 97008 (QUE 97008; LL 3.05). In ALHA77307, the only silicates we analyzed for their nickel isotope composition were olivine chondrule fragments with no age information. In case of the UOCs, we analyzed silicates in four chondrules. The age of three of these chondrules relative to CCAIs was estimated from their magnesium isotope composition and Al/Mg ratios.

Analytical methods: All analytical work discussed below took place in the Max Planck Institute for Chemistry (Mainz, Germany). Isotope measurements were carried out with the NanoSIMS.

Selection of objects for isotope analyses. Back-scattered electron images together with X-ray point analyses and element maps (LEO1530 scanning electron microscope; Oxford X-Max 80 mm² energy dispersive X-ray detector) were used to choose spots in iron-rich, but nickel-poor silicates for NanoSIMS iron-nickel analysis, and to find chondrule phases with a high Al/Mg ratio (i.e., ≥ ~50) for Al-Mg dating.

Measurement of Al/Mg and magnesium isotope ratios. 6 × 6 µm² areas of calcic plagioclase were scanned with a ~12 pA, ~0.2 µm diameter $^{16}O^-$ primary ion beam, while positive secondary ions of ^{24}Mg, ^{25}Mg, ^{26}Mg, ^{27}Al, and ^{28}Si were collected simultaneously on electron multipliers (EMs). Signals were integrated over the central 4 × 4 µm² area of each spot, to minimize the effect of isotope fractionation on crater edges. San Carlos and chondrule olivine (magnesium isotope ratios) and NIST SRM611 silicate glass (Al/Mg ratios) were used as external standards. Measured ^{25}Mg/^{24}Mg ratios were used for internal normalization. Magnesium isotope data were corrected for the quasi-simultaneous-arrival effect [10], to avoid spurious "^{26}Mg-enrichments", resulting from the much higher count rates of magnesium/primary ion intensity in olivine, than in plagioclase.

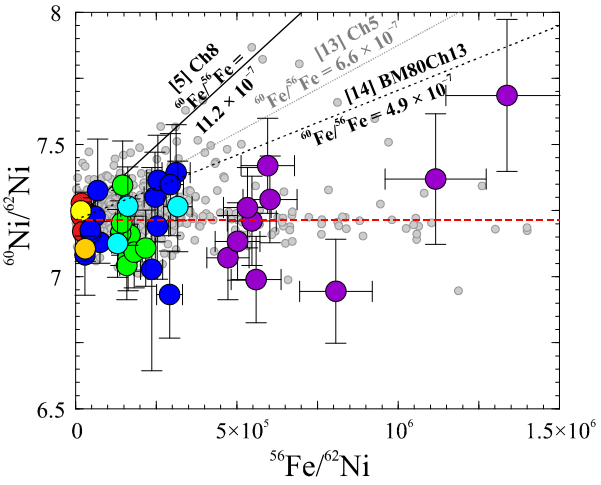

Figure 1. *$^{56}Fe/^{62}Ni$ and $^{60}Ni/^{62}Ni$ ratios of chondritic silicates. Colored symbols: own data with uncertainties (1 σ). Each color represents a different chondrule or chondrule fragment. Gray symbols: literature data ([5,12–14]) without uncertainties, for legibility. For reference, lines corresponding to some of the highest $^{60}Fe/^{56}Fe$ ratios inferred before for individual chondrules are also indicated, as is the terrestrial $^{60}Ni/^{62}Ni$ ratio (red dashed line).*

Measurement of Fe/Ni and nickel isotope ratios. We chose olivine, enstatite, and non-stoichiometric, cryptocrystalline silicate material for iron and nickel isotope analysis, and measured several points in all chondrules and most chondrule fragments. Typically, on each point, a $^{16}O^-$ primary ion beam of ~100 or ~500 pA intensity and 0.2–1.0 µm diameter was scanned over a square with 3 × 3 µm² nominal area, while the resulting positive secondary ions of ^{29}Si, ^{46}Ti, ^{54}Fe, ^{60}Ni, and ^{62}Ni were collected simultaneously, and counted by EMs. Most measurements were performed in imaging mode, with the inner 2 × 2 µm² of the images used for signal integration. Imaging enabled the identification of nickel- or iron-rich cracks or inclusions, which were left out of signal integration. We used San Carlos olivine and an in-house terrestrial enstatite as external standards. (We note, however, that our test measurements showed raw $^{60}Ni/^{62}Ni$ ratios on both standards to be identical on the few-permil level, despite the order-of-magnitude difference in Fe/Ni ratios and nickel count rates.)

Results and Discussion: The three dated chondrules formed 1.51 +0.25/−0.20, 2.1 +1.5/−0.6, and 1.13 +0.23/−0.19 million years (Ma) after CCAIs. Thus, they are probably older than the majority of UOC chondrules (frequency peak between 2 and 2.3 Ma after CCAIs; [11]), a circumstance advantageous when fossil ^{60}Fe is to be detected.

$^{56}Fe/^{62}Ni$ ratios, calculated from measured ^{54}Fe and ^{62}Ni counts, range from 16,770 ± 250 to 1,340,000 ± 190,000 in the analyzed silicates. The frequency of data points decreases drastically above $^{56}Fe/^{62}Ni \approx$ 300,000. The range and distribution of our $^{56}Fe/^{62}Ni$ data are thus similar to what was reported previously by in situ studies (Fig. 1). $^{60}Fe/^{56}Fe$ ratios at formation were estimated by linear regression of the data in the $^{60}Ni/^{62}Ni$ vs. $^{56}Fe/^{62}Ni$ space, following [15], except for chondrule QUE97008_b16. For this chondrule, the weighted averages of $^{60}Ni/^{62}Ni$ and $^{56}Fe/^{62}Ni$ ratios were used for the estimation of $^{60}Fe/^{56}Fe$, because measured $^{56}Fe/^{62}Ni$ ratios were identical within analytical uncertainty (1 σ). Estimated $^{60}Fe/^{56}Fe$ ratios of chondrules and chondrule fragments range from $-6.8\ (\pm 5.8) \times 10^{-6}$ to $5.1\ (\pm 9.8) \times 10^{-7}$, and are all 0 within 2 σ. The best constrained $^{60}Fe/^{56}Fe$ is that of chondrule Ch1 from MET 00526 $(7.8\ (\pm 33.8) \times 10^{-8}$; $\chi^2 = 0.69)$. From the age of this chondrule (1.51 +0.25/−0.20 Ma after CCAIs), a $^{60}Fe/^{56}Fe_{CCAI}$ of 1.2 $(\pm 5.1) \times 10^{-7}$ can be estimated. Our UOC dataset as a whole yields 1.4 $(\pm 10.7) \times 10^{-8}$ for average $^{60}Fe/^{56}Fe$.

Conclusions and outlook: We have not found evidence for in situ ^{60}Fe decay in chondritic silicates, even though some of them appear to be old enough, and have large enough Fe/Ni ratios, to produce an enrichment in ^{60}Ni detectable with the NanoSIMS, provided $^{60}Fe/^{56}Fe_{CCAI}$ ratios estimated previously based on in situ measurements (~10^{-6}; see above and Fig. 1) are accurate. We plan to perform further isotope analyses, and investigate using TEM, if potential element re-distribution or recrystallization occurred in our apparently fossil ^{60}Fe-free samples.

Acknowledgments: We are grateful for the technical help of Elmar Gröner and Philip Schumann. The samples were kindly provided by NASA JSC. Our project is supported by the German Research Foundation (DFG; grant numbers HO2163/3-1 and VO1816/4-1; Special Priority Program 1833).

References: [1] Rugel G. et al. (2009) *PRL, 103*, 072502. [2] Tang H. and Dauphas N. (2015) *ApJ, 802*, 22. [3] Jacobsen B. et al. (2008) *EPSL, 272*, 353–364. [4] Steele R. C. J. et al. (2012) *ApJ, 758*, 59. [5] Mishra R. K. and Goswami J. N. (2014) *GCA, 132*, 440–457. [6] Mostefaoui S. et al. (2005) *ApJ, 625*, 271–277. [7] Elliott T. and Steele R. C. J. (2017) *Rev. Mineral. Geochem., 82*, 511–542. [8] Telus M. et al. (2016) *GCA, 178*, 87–105. [9] Kodolányi J. et al. (2019) *82nd Annual Meeting of The Meteoritical Society*, Abstract #6373. [10] Slodzian G. et al. (2004) *Appl. Surf. Sci., 231–232*, 874–877. [11] Pape J. et al. (2019) *GCA, 244*, 416–436. [12] Mishra R. K. and Chaussidon M. (2014) *EPSL, 398*, 90–100. [13] Mishra R. K. et al. (2016) *EPSL, 436*, 71–81. [14] Telus M. et al. (2018) *GCA, 221*, 342–357. [15] Mahon K. I. (1996) *Intl. Geol. Rev., 38*, 293–303.